
HOKKAIDO UNIVERSITY

Title	Efficient synthesis of α-galactosyl oligosaccharides using a mutant Bacteroides thetaiotaomicron retaining α-galactosidase (BtGH97b)
Author(s)	Okuyama, Masayuki; Matsunaga, Kana; Watanabe, Ken-ichi; Yamashita, Keitaro; Tagami, Takayoshi; Kikuchi, Asako; Ma, Min; Klahan, Patcharapa; Mori, Haruhide; Yao, Min; Kimura, Atsuo
Citation	FEBS Journal, 284(5), 766-783 https://doi.org/10.1111/febs.14018
Issue Date	2017-03
Doc URL	http://hdl.handle.net/2115/68390
Rights	This is the peer reviewed version of the following article: FEBS Journal 284(5), pp766-783, 2017, which has been published in final form at 10.1111/febs.14018. This article may be used for non-commercial purposes in accordance with Wiley Terms and Conditions for Self-Archiving.
Type	article (author version)
File Information	Main_text_v2.pdf


Instructions for use

Hokkaido University Collection of Scholarly and Academic Papers : HUSCAP

Efficient synthesis of α-galactosyl oligosaccharides using a mutant *Bacteroides thetaiotaomicron* retaining α-galactosidase (*Bt*GH97b)

Masayuki Okuyama [1], Kana Matsunaga [1], Ken-ichi Watanabe [1], Keitaro Yamashita [2], Takayoshi Tagami [1], Asako Kikuchi [1], Min Ma [1], Patcharapa Klahan [1], Haruhide Mori [1], Min Yao [2], and Atsuo Kimura [1]

1. Laboratory of Molecular Enzymology, Research Faculty of Agriculture, Hokkaido University; Kita-9, Nishi-9, Kita-ku, Sapporo, Hokkaido 060-8589, Japan
2. Laboratory of X-ray Structural Biology, Faculty of Advanced Life Science, Hokkaido University; Kita-10, Nishi-8, Kita-ku, Sapporo, Hokkaido 060-0810, Japan

Corresponding author: Prof. Atsuo Kimura, Laboratory of Molecular Enzymology, Research Faculty of Agriculture, Hokkaido University; Kita-9, Nishi-9, Kita-ku, Sapporo, Hokkaido 060-8589, Japan. Telephone: +81-11-706-2808; Fax: +81-11-706-2808; E-mail: kimura@abs.agr.hokudai.ac.jp

Running Title: Chemical-rescued transfer and structure of *Bt*GH97b

Abbreviations: α-GalF, α-galactopyranosyl fluoride; Gal-Lac, β-lactosyl α-D-galactopyranoside; GH, glycoside hydrolase family; HMBC, heteronuclear multiple bond correlation; HPAEC–PAD, high-performance anion exchange chromatography–pulsed amperometric detection.

Enzymes: α-galactosidase (EC 3.2.1.22)

Database: The atomic coordinates (code: 5E1Q) has been deposited in the Protein Data Bank.

Keywords: carbohydrate synthesis, chemical rescue, crystal structure, enzyme kinetics, glycoside hydrolase

Conflict of interest: The authors declare that they have no conflicts of interest resulting from the contents of this article.

Abstract

The preparation of a glycosynthase, a catalytic nucleophile mutant of a glycosidase, is a well-established strategy for the effective synthesis of glycosidic linkages. However, glycosynthases derived from α-glycosidases can give poor yields of desired products because they require generally unstable β-glycosyl fluoride donors. Here, we investigate a transglycosylation catalyzed by a catalytic nucleophile mutant derived from a glycoside hydrolase family (GH) 97 α-galactosidase, using more stable β-galactosyl azide and α-galactosyl fluoride donors. The mutant enzyme catalyzes the glycosynthase reaction using β-galactosyl azide and α-galactosyl transfer from α-galactosyl fluoride with assistance of external anions. Formate was more effective at restoring transfer activity than azide. Kinetic analysis suggests that poor transglycosylation in the presence of the azide is because of low activity of the ternary complex between enzyme, β-galactosyl azide, and acceptor. A three-dimensional structure of the mutant enzyme in complex with the transglycosylation product, β-lactosyl α-D-galactoside, was solved to elucidate the ligand-binding aspects of the α-galactosidase. Subtle differences at the β→α loops 1, 2, and 3 of the catalytic TIM barrel of the α-galactosidase from those of a homologous GH97 α-glucoside hydrolase seem to be involved in substrate recognitions. In particular, the Trp residues in β→α loop 1 have separate roles. Trp312 of the α-galactosidase appears to exclude the equatorial hydroxy group at C4 of glucosides, whereas the corresponding Trp residue in the α-glucoside hydrolase makes a hydrogen bond with this hydroxy group. The mechanism of α-galactoside-recognition is conserved among GH27, 31, 36, and 97 α-galactosidases.

Introduction

Carbohydrates are involved in a range of important biological processes and there is an increasing need to synthesize compounds containing carbohydrates and their analogues. Almost all oligosaccharides are synthesized *in vivo* by Leloir glycosyltransferases and these enzymes can be exploited for the *in vitro* synthesis of oligosaccharides in high yield. However, glycosyltransferases require costly and poorly available sugar nucleotides as glycosyl donors.

Retaining glycosidases catalyze the hydrolysis of *O*-glycosidic linkages *via* a double displacement mechanism, and can be used for the formation of glycosidic linkages. This reaction, so-called transglycosylation, is often used for the production of the glycosidic linkages because it can be undertaken using an inexpensive and readily available glycosyl donor. Ensuring maximal transglycosylation product yield is challenging because the product can be hydrolyzed by the retaining glycosidase. This problem can be overcome by converting the glycosidase into a glycosynthase [1,2]. A glycosynthase can be easily made by removing the nucleophile catalyst in the active site. A glycosynthase is capable of catalyzing glycosyl transfer from a glycosyl fluoride—with the opposite anomeric configuration of the natural substrate—to the acceptor molecule. Eliminating the nucleophile of the enzyme abolishes the hydrolytic activity and prevents product degradation. Glycosynthases are thus valuable resources for oligosaccharide syntheses. However, instability of glycosyl fluoride donors sometimes becomes a bottleneck for this synthetic approach. The donor substrates of glycosynthases derived from α-glycosidases are unstable β-glycosyl fluorides. These donors spontaneously hydrolyze, prohibiting high yield syntheses of desired products [3]. Indeed, the yields of oligosaccharides catalyzed by a glycosynthase derived from an α-glucosidase were lower than those catalyzed by other glycosynthases [4]. Cobucci-Ponzano *et al*. used a β-glycosyl azide in place of an unstable β-glycosyl fluoride—because the azide is more stable than the β-glycosyl fluoride—as the donor substrate for glycosynthases derived from glycoside hydrolase family 36 (GH36) α-galactosidase and GH29 α-L-fucosidase, and succeeded in the formation of α-galactosidic and α-L-fucosidic linkages [5,6]. Apart from the glycosynthase, Moracci and colleagues [7] established an alternative method for oligosaccharide syntheses using a nucleophile mutant of a β-glycosidase in combination with an external nucleophilic anion. The catalytic activity of nucleophile mutants are generally rescued by an anion such as azide, formate, or acetate. The anion takes the role of the catalytic nucleophile and attacks the anomeric carbon of the glycoside to promote departure of a leaving group and forms an inverted glycoside [8]. Moracci *et al.* [7] found that the inverted glycoside acted as a donor substrate that transferred to a suitable acceptor molecule. The products were not hydrolyzed because the external anion was only effective against substrates that possess a good leaving group.

In this study, we investigated the use of a glycosynthase with β-galactosyl azide (β-GalN_3)

and the chemical-rescued transglycosylation for the synthesis of α-galactosyl oligosaccharides, using a nucleophile mutant enzyme derived from *Bacteroides thetaiotaomicron* glycoside hydrolase family (GH) 97 retaining α-galactosidase (*Bt*GH97b). These procedures allowed us to use the relatively stable α-galactosyl fluoride (α-GalF) and β-$GalN_3$ as donor substrates for oligosaccharide syntheses, instead of the labile β-galactosyl fluoride. We studied the transglycosylation kinetics using lactose as an acceptor molecule. This is because we aim to make α-galactosyl carbohydrates that are useful in therapeutic applications, such as the α-Gal epitope [α-Gal-(1→3)-β-Gal-(1→4)-GlcNAc-R] and globosyl-Gb2/Gb3 [α-Gal-(1→4)-β-Gal-R/α-Gal-(1→4)-β-Gal-(1→4)-β-Glc-R]. We confirmed that transglycosylation with the assistance of formate was the best strategy among the three methods tested for the synthesis of oligosaccharides. Azide can rescue the donor cleavage reaction better than formate. However, an accumulation of β-galactosyl azide was observed and the yield of the transfer product was lower than that of the formate-assisted transglycosylation. A kinetic study suggested the formation of a less active ternary complex between enzyme, β-galactosyl azide, and acceptor. The kinetic evaluation of acceptor specificity in the formate-rescued transglycosylation shall also be discussed. Furthermore, we solved a crystal structure of the nucleophile mutant enzyme of *Bt*GH97b (*Bt*GH97b-D415G) complexed with a transglycosylation product. GH97 is a unique family that contains inverting and retaining enzymes [9,10]. The inverting enzyme (*Bt*GH97a) selectively hydrolyzes non-reducing terminal α-glucosidic linkages in *p*-nitrophenyl (PNP) and 2,4-dinitrophenyl α-glucopyranosides, α-glucobioses, and maltooligosaccharides. The crystal structure of acarbose-binding *Bt*GH97a has been determined and allows us to understand its substrate-binding aspects [9,10]. The retaining enzyme, *Bt*GH97b, definitely recognizes and hydrolyzes non-reducing terminal α-galactosidic linkages including PNP α-galactopyranoside and melibiose [α-galactopyranosyl-(1→6)-glucopyranoside], and seldom acts on α-glucosidic linkages [9–11]. The structure determined is ligand free and there is no information about the α-galactoside-binding site of *Bt*GH97b [11]. The structure determined in this study provides a difference in substrate recognition from *Bt*GH97a and similarity to α-galactosidases of other GHs.

Results

Chemical-rescued transglycosylations with *Bt*GH97b-D415G

The chemical-rescued reaction rates were measured with 20 mM α-GalF as the substrate. The initial velocity of fluoride ion release without any external nucleophile was 0.0547 s^{-1} (= $v/[E]_0$). Addition of formate or azide ions raised the velocity, which increased by 180% with 100 mM sodium formate or by 4,000% with 300 mM sodium azide (Fig. 1). Greater concentrations of the external anions did not cause further increases in the velocity.

Transglycosylation by *Bt*GH97b-D415G in the presence of an external anion was investigated. An equimolar ratio of α-GalF and lactose (20 mM each) was incubated with 100 mM sodium formate, sodium azide, or sodium acetate. The reaction mixtures were analyzed by thin-layer chromatography (TLC) and high-performance anion exchange chromatography–pulsed amperometric detection (HPAEC–PAD) after a 48-h incubation (Fig. 2). The transglycosylation product was detected by TLC when formate was used as the external nucleophile (Fig. 2A). The product concentration amounted to 12 mM at 24 h and remained unchanged after 48 h (Fig. 2B). Sodium acetate and sodium azide were ineffective in rescuing transglycosylation activity and failed to produce the desired product, with the accumulation of β-galactosyl azide observed when azide was used as the external nucleophile (Fig. 2B). The appropriate ratio of donor and acceptor was explored using lactose as the acceptor. The use of an equimolar ratio of α-GalF and lactose (20 or 40 mM) resulted in incomplete consumption of the lactose. The use of 40 mM α-GalF and 20 mM lactose gave almost complete consumption of lactose after a 48-h incubation. To explore the scope of saccharide acceptors, six monosaccharides (20 mM glucose, xylose, fructose, mannose, galactose, or talose), and four disaccharides (20 mM maltose, cellobiose, lactose, or sucrose), were individually incubated with 40 mM α-GalF, *Bt*GH97b-D415G, and 100 mM sodium formate. The reaction mixtures were analyzed using TLC after 48-h incubations (data not shown). Glucose, xylose, maltose, cellobiose, and lactose were able to act as acceptors, but the other carbohydrates did not form new glyosidic linkages. Several products were detected when glucose, xylose, maltose and cellobiose were used as acceptors. It was difficult to determine each product concentration and the yields of transglycosylation products from their effective saccharides, but progress of each reaction was readily estimated from the consumption of acceptor molecules (Table 1). A single trisaccharide species was produced when lactose was used as the acceptor molecule, and thus the efficiency of transglycosylation *versus* hydrolysis was calculated

by determining the concentration of the transfer product and galactose. α-GalF (40 mM) and lactose (20 mM) were incubated in the presence of 100 mM sodium formate for 48 h and the reaction mixture was separated by HPLC. The concentration of the product, galactose, and α-GalF were 17, 19, and 4 mM, respectively. The transglycosylation product thus comprised 47% of the reaction carbohydrates. The yield estimated from the consumption of acceptor molecule was 85% (Table 1). In addition, we tested whether PNP glycosides were suitable as acceptor molecules. Each PNP glycoside (10 mM α-glucoside, β-glucoside, α-mannoside, β-mannoside, α-galactoside, or β-galactoside) was incubated with 20 mM α-GalF, *Bt*GH97b-D415G, and 100 mM sodium formate. The reaction mixtures were subjected to reverse-phase HPLC to estimate the concentrations of the products. PNP α- and β-glucosides and PNP α- and β-mannosides were able to act as acceptors but PNP α- and β-galactosides were not. Product yields were calculated as follows: 95%, PNP α-glucoside; 89%, PNP β-glucoside; 92%, PNP α-mannoside; and 73%, PNP β-mannoside (Table 1).

The chemical-rescued transglycosylation in the presence of 300 mM sodium azide was also investigated. The yield of the transglycosylation products were estimated as per the methods used for the formate-rescue reactions (Table 1). The yields in the azide-rescued transglycosylations were lower than those of the formate-rescued reactions. Consumption of lactose was hardly observed and this disaccharide was demonstrated to be a less effective acceptor molecule in the azide-rescued reaction. The reaction mixture consisting of 40 mM α-GalF, 20 mM lactose, *Bt*GH97b-D415G, and 300 mM sodium azide was analyzed using HPLC after a 48-h incubation. The concentration of the transfer product, galactose, β-$GalN_3$, and α-GalF were 0.7, 10, 27 and 2.2 mM, respectively. Around 70% of the whole reaction proved to end at the β-$GalN_3$ intermediate.

Glycosynthase using β-$GalN_3$ as the donor substrate

The glycosynthase reaction of *Bt*GH97b-D415G using 20 mM β-$GalN_3$ as a donor substrate was investigated. Five natural carbohydrates (20 mM glucose, xylose, maltose, cellobiose, or lactose) were individually incubated with *Bt*GH97b-D415G and 20 mM β-$GalN_3$. The yields of the transglycosylation products from these saccharides were estimated from the consumption of acceptor molecule (Table 1). PNP α- and β-glucosides and PNP α- and β-mannosides (10 mM)

were also incubated with the enzyme and 10 mM β-$GalN_3$. Each reaction mixture was subjected to HPLC analysis after 48 h and the yields of the products from the PNP glycosides were calculated (Table 1). Every reaction synthesized new glycoside(s), with yields of 16% to 47%. These results indicated that *Bt*GH97b-D415G successfully catalyzed the glycosynthase reaction using β-$GalN_3$ as a donor substrate. Transglycosylation kinetics with *Bt*GH97b-D415G using β-$GalN_3$ and lactose as donor and acceptor substrates, respectively, were investigated using a HPAEC–PAD to monitor the α-galactosyl lactose production. The plots of velocities *versus* [β-$GalN_3$] at a fixed concentration of lactose (100 mM) displayed standard Michaelis–Menten kinetics (Fig. 3A), with apparent kinetic parameters of K_m = 0.21 ± 0.04 mM, k_{cat} = 0.089 ± 0.004 s^{-1}, and k_{cat}/K_m = 0.423 s^{-1} mM^{-1}. The velocities of product release at various lactose concentrations under a fixed concentration of β-$GalN_3$ (10 mM) also displayed standard saturation kinetics (Fig. 3B), with apparent kinetic parameters of K_m = 52 ± 3 mM, k_{cat} = 0.064 ± 0.002 s^{-1}, and k_{cat}/K_m = 0.0012 s^{-1} mM^{-1}.

Structures of transglycosylation products

The transfer products were identical among all reactions with homologous substrates and acceptors. The products from reactions using α-GalF in the presence of formate ion were isolated by HPLC and the main products were subjected to structural analyses. Using glucose as the acceptor generated one major and three minor products. Electrospray ionization-mass spectrometry (ESI-MS) revealed that the major product (*m*/*z* 365.10 for $C_{12}H_{22}O_{11}$ + Na^+) and one minor product (*m*/*z* 365.11 for $C_{12}H_{22}O_{11}$ + Na^+) were disaccharides, and the other two minor saccharides (*m*/*z* 527.16 for $C_{18}H_{32}O_{16}$ + Na^+) were trisaccharides. The trisaccharides are likely formed from further reactions of the disaccharide products. ^{1}H- and ^{13}C-NMR spectra of the major disaccharides were assigned using two-dimensional NMR, unveiling the product as a non-reducing sugar, β-D-glucopyranosyl α-D-galactopyranoside [α-D-Gal*p*-(1↔1) β-D-Glc*p*]. The formation of the α-(1↔1)-β linkage was confirmed by the presence of a correlation between H-1 (coupling constant, *J* = 7.6 Hz) of the glucose residue and C-1 of the galactose residue, and the correlation between H-1 (*J* = 3.4 Hz) of the galactose residue and C-1 of the glucose residue in the heteronuclear multiple bond correlation (HMBC) spectrum (Fig. 4A).

Xylose was converted to one major disaccharide product (ESI-MS: *m*/*z* 335.1 for $C_{11}H_{20}O_{10}$

+ Na^+) and two minor trisaccharide products (ESI-MS: *m*/*z* 497.2 for $C_{17}H_{30}O_{15}$ + Na^+). ^{1}H- and ^{13}C-NMR, together with two-dimensional NMR experiments, identified the major disaccharide as α-D-galactopyranosyl-(1→4)-D-xylopyranose [α-D-Gal*p*-(1→4) D-Xyl*p*], with the α-(1→4) linkage supported by the correlation between H-4 and C′-1 in the HMBC spectrum (Fig. 4B).

A single trisaccharide species (ESI-MS: *m*/*z* 527.16 for $C_{18}H_{32}O_{16}$ + Na^+) was produced when lactose was used as the acceptor molecule. The NMR spectra indicated that the trisaccharide was β-lactosyl α-D-galactopyranoside [α-D-Gal*p*-(1↔1)-β-D-Glc*p*-(4←1)β-D-Gal*p*; Gal-Lac], which respective occupancies of β-glucosyl and β-galactosyl moieties at subsites +1 and +2 formed. The α-(1↔1)-β linkage was determined by the HMBC-correlation between H-1 (*J* = 8.2 Hz) of the glucose residue and C-1 of the galactose residue, and that between H-1 (*J* = 3.8 Hz) of the galactose residue and C-1 of the glucose residue (Fig. 4C).

The reaction with maltose as the acceptor formed one major and two minor trisaccharide (ESI-MS: *m*/*z* 527.16 for $C_{18}H_{32}O_{16}$ + Na^+), and three minor tetrasaccharide (ESI-MS: *m*/*z* 689.21 for $C_{24}H_{42}O_{21}$ + Na^+) products. The major trisaccharide was subjected to ^{1}H-NMR analysis. Three doublet signals with similar integrated values were detected at δ=5.40 (*J* = 3.4 Hz), δ=5.27 (*J* = 3.4 Hz), and δ=4.65 ppm (*J* = 8.2 Hz), respectively, and no other notable doublet signals were detected in the anomeric region (Fig. 4D). This result implied that the trisaccharide has three anomeric protons with α, α, and β anomeric configurations, respectively, and is the non-reducing sugar, β-maltosyl α-D-galactopyranoside [α-D-Gal*p*-(1↔1)-β-D-Glc*p*-(4←1)α-D-Glc*p*].

The formation of two saccharides from cellobiose was confirmed by HPLC. ESI-MS revealed that the major product was a trisaccharide (*m*/*z* 527.16 for $C_{18}H_{32}O_{16}$ + Na^+) and another minor product was a tetrasaccharide (*m*/*z* 689.21 for $C_{24}H_{42}O_{21}$ + Na^+). ^{1}H-NMR analysis of the major product isolated by HPLC showed seven anomeric proton doublet signals: δ=5.27 (*J* = 3.8 Hz), δ=5.22 (*J* = 3.8 Hz), δ=5.01 (*J* = 3.8 Hz), δ=4.68 (*J* = 7.7 Hz), δ=4.66 (*J* = 7.7 Hz), δ=4.54 (*J* = 8.0 Hz), and δ=4.51 (*J* = 8.0 Hz) (Fig. 5A). This suggests that the single HPLC peak contained two trisaccharides, a non-reducing sugar and a reducing sugar having three and four anomeric proton signals, respectively. Further attempts to separate these species were unsuccessful. A β-glucosidase hydrolysis and a methylation analysis were employed to determine the linkages of the two saccharide products. Treatment of the mixture of two saccharides with β-glucosidase gave peaks in the HPLC analysis for glucose, α-Gal-(1↔1)β-Glc, and a persistent

original sugar (Fig. 5B). The persistent sugar peak remained without any decrease in peak-area after a 96-h treatment with β-glucosidase, showing that the mixture contains a β-glucosidase-insensitive oligosaccharide. The enzyme certainly hydrolyzes β-Glc-(1→4)-β-Glc linkages, and the results suggest that the mixture contains non-reducing α-D-Gal*p*(1↔1)β-D-Glc*p*-(4←1)β-D-Glc*p* resulting from binding of the reducing and non-reducing ends of glucose moieties of acceptor cellobiose at subsites +1 and +2, respectively. The unhydrolyzed oligosaccharide was subjected to methylation analysis. 2,3,4,6-tetra-*O*-methyl-galactose, 2,3,4-tri-*O*-methyl-glucose, and 2,3,6-tri-*O*-methyl-glucose were detected by TLC (Fig. 5C), suggesting that the resistant oligosaccharide was α-Gal-(1→6)-β-Glc-(1→4)-Glc. This compound was formed when the hydroxy group at C6 of the glucose moiety of non-reducing end of cellobiose attacked the anomeric carbon of the β-galactosyl formate intermediate.

The glycosidic linkages of the transfer products using PNP glucosides as acceptor molecules were examined by methylation analysis. The analyses suggested that reactions formed α-(1→6) glycosidic linkages.

Kinetic analysis of the chemical-rescued transglycosylation

Kinetic parameters of the reaction by *Bt*GH97b-D415G in the presence of 100 mM sodium formate or 300 mM sodium azide were determined with or without lactose (Table 2). The initial velocities of fluoride ion release from various concentrations of α-GalF as the sole substrate were measured. The plots of velocities *versus* [α-GalF] exhibited standard Michaelis–Menten behavior in each condition (Fig. 6A, B). The k_{cat} and k_{cat}/K_m values in the presence of 300 mM sodium azide were significantly higher than those in the presence of 100 mM sodium formate. The effect of adding 100 mM of lactose on the reaction velocity was next investigated. Addition of 100 mM lactose did not affect the Michaelian kinetic behavior. The addition of 100 mM lactose slightly increased K_m and k_{cat} values in the presence of 100 mM sodium formate, with little effect on k_{cat}/K_m. Lactose addition significantly decreased the k_{cat} and k_{cat}/K_m values in the presence of 300 mM sodium azide. The transglycosylation of *Bt*GH97b-D415G with the assistance of the external nucleophile can follow the reaction scheme shown in Fig. 7. The enzyme should form the dead-end ES_2 complex, which is generated by the binding of the lactose molecule (S_2) to the free enzyme (E), because k_{cat}/K_m was affected by the presence of lactose. The other possible dead-end

species, including ESS_2 (enzyme · α-GalF · lactose) and $ES'S_2$ (enzyme · β-galactosyl azide · lactose) ternary complexes, never affect k_{cat}/K_m. Solving this scheme by applying the steady state assumption to [ES], [ES′], and [ES′S_2] gave equation 1:

$$\frac{v_{P1}}{[E]_0} = \frac{\dfrac{\dfrac{k_2 k_3}{k_2+k_5}K_{m2} + \dfrac{k_2 k_5}{k_2+k_5}[S_2]}{\dfrac{k_2+k_3}{k_2+k_5}K_{m2} + [S_2]} \cdot [S]}{K_{m1}\left(1+\dfrac{[S_2]}{K_{S2}'}\right)\dfrac{(k_3 K_{m2} + k_5[S_2])}{(k_2+k_3)K_{m2} + (k_2+k_5)[S_2]} + [S]}, \qquad \text{Equation 1}$$

where K_{S2}' is a disassociation constant of ES_2, $K_{m1} = (k_{-1} + k_2)/k_1$, and $K_{m2} = (k_{-4} + k_5)/k_4$.

Equation 1 follows a simple Michaelis–Menten rate equation when the concentration of α-GalF [S] varies under a fixed lactose concentration [S_2], and k_{cat}/K_m can be expressed as follows:

$$\frac{k_{cat}}{K_m} = \frac{k_2}{K_{m1}\left(1+\dfrac{[S_2]}{K_{S2}'}\right)}$$

K_{S2}' was estimated to be 13.3 mM in the presence of azide. In the presence of formate, a decrease in k_{cat}/K_m was not observed and $K_{s2}' \gg [S_2]$ (= 100 mM) should hold. Kinetic parameters were determined with varying concentrations of lactose under fixed concentrations of α-GalF (10 mM) and an external nucleophile (100 mM sodium formate or 300 mM sodium azide). The velocity of fluoride ion release at various lactose concentrations in the presence of formate displayed a saturation curve, which did not pass through the origin (Fig. 6C). The velocity decreased in the presence of azide with increasing lactose concentration (Fig. 6D). The α-GalF concentration (10 mM) used was deemed to be greater than K_m (K_m = 0.136 mM with formate, K_m = 0.101 mM with azide; Table 2) and the relevant enzyme species were regarded as ES, ES′, and ES′S_2 ($[E]_0$ = [ES] + [ES′] +[ES′S_2]). In this case, equation 1 can be simplified to equation 2.

$$\frac{v}{[E]_0} = \frac{\alpha + \beta[S_2]}{\gamma + [S_2]} \quad \text{Equation 2}$$

where $\alpha = k_2k_3K_{m2}/(k_2 + k_5)$ $\beta = k_2k_3K_{m2}/(k_2 + k_5)$, and $\gamma = (k_2 + k_3)K_{m2}/(k_2 + k_5)$.

The initial velocities under varying [lactose] with a fixed [α-GalF] fit well to equation 2. These kinetic results, v – [α-GalF] and v – [lactose] under the fixed [lactose] and [α-GalF], respectively, suggested that the chemical-rescued transglycosylation of *Bt*GH97b-D415G followed the scheme in Fig. 7.

The initial velocity of the formate ion-mediated reaction was also measured with alternative acceptor substrates, including galactose, glucose, xylose, maltose, and cellobiose. These acceptors followed equation 2 with the exception of galactose, with no increase in the velocity of fluoride release observed for galactose. The constants α, β, and γ for the glycosyl acceptors are summarized in Table 3.

Crystal structure of *Bt*GH97b-D415G complexed with Gal-Lac

The crystal structure of *Bt*GH97b-D415G complexed with Gal-Lac was determined at 1.9 Å resolution (Fig. 8A). The structure was almost identical with the free wild-type enzyme with root mean square deviations (r.m.s.d.) of 0.20 Å for 641 Cα atoms, indicating that the mutation had no noticeable effect on the three-dimensional structure of the protein. The mutation of Asp415 to Gly made a cavity that was sufficient to accommodate the formate or azide ion. A calcium ion, characteristic of GH97 enzymes, and Gal-Lac were located at the active site (Fig. 8B). In the ligand-free wild-type enzyme [11], the calcium ion was bound to three glutamate residues (Glu174, Glu464, and Glu470) and four water molecules with a pentagonal bipyramid geometry. In the *Bt*GH97b-D415G-Gal-Lac complex, three of the four water molecules were replaced by hydroxyl groups and the α-galactosidic oxygen of Gal-Lac (Fig. 8C). The α-galactosyl moiety at subsite −1 made several important contacts with the protein and the calcium ion (Fig. 8C). Hydrogen bonds were formed between the O3 atom and Lys413 and His445, and between the O2 atom and His445 and Glu464. The O2 atom also interacted with the calcium ion. These features were similar to the ligand-binding structures of *Bt*GH97a [9,10]. The axial O4 atom was

recognized through hydrogen bonds to Asp350, Lys413, and Trp387. The indole ring of Trp312 stacked with the hydrophobic face of the galactose ring, which is composed of C4, C5, and C6. The O6 atom was hydrogen bonded to Glu351 and O6 of the β-glucose moiety. Subsite +1 leading out to the entrance of the active-site pocket was narrow, owing to His245, Trp312, Phe416, Glu470, and Trp474 (Fig. 8D). The β-glucosyl moiety at subsite +1 was tightly surrounded by these amino-acid residues, and the carboxy group of Glu174 established a hydrogen bond with the O2 atom (Fig. 8C, D). The β-galactosyl moiety at subsite +2 was juxtaposed to the indole ring of Trp474 (Fig. 8D).

Discussion

It is difficult to use an orthodox glycosynthase to synthesize an α-galactoside because of the instability of β-galactosyl fluoride. In this study, we tested other known procedures for making α-galactosides using a catalytic nucleophile mutant of GH97 α-galactosidase, *Bt*GH97b-D415G. The enzyme catalyzed both an alternative glycosynthase reaction using β-GalN_3 as the donor substrate and the transfer reaction with the assistance of an external formate or azide ion nucleophile. The transfer reaction in the presence of the formate ion was the most efficient procedure of the three methods investigated. We performed kinetic analyses of the transfer reactions using lactose as an acceptor molecule. This is because we are interested in making α-galactosyl carbohydrates that have uses in therapeutic processes, such as the α-gal epitope and globosyl-Gb2/Gb3, although the transfer reaction resulted in the formation of a non-reducing trisaccharide. The kinetic study suggests that the low reactivity of the glycosyl-azide intermediate is involved in the limited transfer reaction in the azide-rescued reaction. The stable β-GalN_3 leads to poor reactivity of the ternary complex of enzyme, β-GalN_3, and lactose, and thus the reaction may progress to liberate β-GalN_3 from the enzyme (E + P_2 in the reaction scheme in Fig. 4). This equated to a k_5 smaller than k_3 in the scheme. The kinetic analysis cannot give the values of these rate constants, but the kinetic constants of equation 2 provide $k_2k_3/(k_2 + k_3)$ and $k_2k_5/(k_2 + k_5)$ values: $k_2k_5/(k_2 + k_5)$ corresponds to β in equation 2 and $k_2k_3/(k_2 + k_3)$ can be calculated by α/γ. We established that $k_2k_3/(k_2 + k_3) > k_2k_5/(k_2 + k_5)$ in the azide-rescued reaction (Table 2), indicating that $k_3 > k_5$ and that the reaction progresses to liberate β-GalN_3 from the enzyme. When formate is used as the external nucleophile, $k_2k_3/(k_2 + k_3)$ is smaller than $k_2k_5/(k_2 + k_5)$, and thus

the formate ion proves to be a suitable external nucleophile for the transfer reaction. Similar results were also observed in a nucleophile mutant of a β-glycosidase and regarded as a consequence of the low reactivity of the glycosyl-azide [7]. In addition, the poor reactivity of the ternary complex (enzyme · β-galactosyl azide · lactose) might result from scarce ability of lactose to act as the acceptor as well as the stabile β-$GalN_3$, because the yield of the product from lactose in the presence of the azide ion was markedly low.

Additional lactose acceptor causes a significant decrease in k_{cat} for the liberation of fluoride from α-GalF in the azide-rescued reaction (Fig. 6B). This might be caused by the stability of the β-galactosyl azide intermediate. From equation 1, the k_{cat} is expressed as follows:

$$k_{cat} = \frac{\frac{k_2 k_3}{k_2 + k_5} K_{m2} + \frac{k_2 k_5}{k_2 + k_5}[S_2]}{\frac{k_2 + k_3}{k_2 + k_5} K_{m2} + [S_2]}$$

The poor reactivity of the ternary complex (enzyme · β-galactosyl azide · lactose) can be regarded as $k_5 \approx 0$ and allows the simplification of the equation to

$$k_{cat} = \frac{\frac{k_2 k_3}{k_2} K_{m2}}{\frac{k_2 + k_3}{k_2} K_{m2} + [S_2]}$$

and

$$\frac{1}{k_{cat}} = \frac{1}{k_2} + \frac{1}{k_3}\left(1 + \frac{[ES'S_2]}{[ES']}\right)$$

This equation indicates that an increase in [ES′S_2], resulting from the poor activity of the ternary complex, causes a decrease in k_{cat}. The decrease in k_{cat}/K_m is observed in the azide-rescued reaction, but not in the formate-rescued reaction, and it appears that K_{S2}' varies depending on the nucleophile species. The glycosynthase kinetics, in which variation of β-$GalN_3$ concentration at a fixed concentration of lactose, follows saturation kinetics and implies that external azide ion is the cause of the formation of ES_2. The reasons why azide ion facilitates the formation of ES_2 are unclear.

Kinetic parameters with varying concentrations of acceptor molecule under fixed concentrations of α-GalF and formate were determined to evaluate acceptor specificity of the transglycosylation. Equation 2 described the kinetics involved and the β/α values (Table 3) can be referred to as a type of specificity constant for the acceptor. The ratio β/α describes the following:

$$\frac{\beta}{\alpha} = \frac{k_4 k_5}{k_{-4} + k_5} \cdot \frac{1}{k_3} \qquad \text{Equation 3}$$

$k_4k_5/(k_{-4} + k_5)$ is a net rate constant for ES′ → ES′S_2 in the reaction of ES′ going to E + P_3 *via* ES′S_2 [12]. Therefore, β/α indicates the partitioning ratio of the rate of ES′ → ES′S_2 to that of ES′ → E + P_2. A high β/α value indicates that ES′ progresses to form ES′S_2 rather than E + P_2. The β/α values for cellobiose and lactose are higher than that for glucose (Table 2), indicating that *Bt*GH97b-D415G prefers disaccharides as acceptor molecules. This result suggests a substantial contribution by subsite +2 to acceptor binding. An indole ring of Trp474 at subsite +2 is likely to play an important role in stabilizing a sugar moiety (Fig. 8D).

The result that PNP α-, and β-mannosides worked as acceptor molecules, but mannose did not, further shows the significance of subsite +2. An interaction between the PNP group and the indole ring of Trp474 may provide sufficient energy for PNP mannosides to act as acceptor molecules. The acceptor specificity and structural features can provide information on substrate specificity of hydrolysis by the wild-type enzyme, i.e., its natural substrate might be the α-galactoside in galactomannan and galactomannooligosaccahrides, which is produced from galactomannan by an action of β-mannanase. In addition, BT2620, a paralogous protein of *Bt*GH97b, has been reported to be responsible for the degradation of α-galactoside in α-mannan [13], and α-mannan may also be a candidate for a natural *Bt*GH97b substrate. *Bt*GH97b-D415G generated non-reducing sugars when lactose, glucose, or maltose were used as the acceptor substrate, and these products have not been identified in nature. The mutant enzyme appears to have produced them incidentally, and this specificity seems not to reflect substrate specificity for the hydrolysis action of the wild-type enzyme. The narrow subsite +1, as mentioned below, may be involved in the formation of the non-reducing sugars.

Subsite +1 appears not to accept a galactose moiety because galactose and PNP α-, and β-galactosides were not suitable acceptors. This can be attributed to the constricted subsite +1 (Fig. 8D). The structure shows that Van der Waals contacts with His245, Trp312, Phe416, and Trp474 are the main binding energy for stabilizing the β-glucosyl moiety at subsite +1. However, these residues narrow the location of subsite +1 and seem to prohibit an axial hydroxy group of galactose from binding. The narrow subsite +1 allows only O1 of a β-glucose (-syl), which has all equatorial hydroxy groups, to react with the β-galactosyl formate. An α-(1→6)-linkage is generated when cellobiose is used as an acceptor (Fig. 5). It is possible that misalignment of the space-restricted subsite +1 and glycosyl moiety occurs when there is a 6-hydroxymethyl group attacking.

The GH97 contains an inverting α-glucoside hydrolase, *Bt*GH97a, and a retaining α-galactosidase, *Bt*GH97b [9,10]. The divergence in catalytic mechanism of these enzymes has been explained by the difference in position of the catalytic residue [11]. However, little is known about how subsite −1 of *Bt*GH97b distinguishes between α-galactosides and α-glucosides, since the structure of *Bt*GH97b has been solved in the substrate-free form [11]. A comparison between structures of *Bt*GH97b and *Bt*GH97a shows that subtle differences are associated with the recognitions of the axial and equatorial hydroxy groups at C4 (Fig. 9A). *Bt*GH97b stabilizes the axial O4 through hydrogen bonds with Asp350, Trp387, and Lys413 on the β→α loops 2, 3, and 4 of the catalytic $(\beta/\alpha)_8$ barrel domain, respectively. *Bt*GH97a has Glu391, His437, and Lys467 residues at equivalent positions [9,10], but their roles in substrate recognition are slightly different: Glu391 contributes to stabilization of an equatorial O4, whereas His437 and Lys467 are involved in the stabilization of O6 and O3, respectively. Coupled with Glu391, Trp331 on the β→α loop 1 is associated with the equatorial O4 through a hydrogen bond. *Bt*GH97b also has Trp312 on the β→α loop 1, but its indole ring is not oriented to form a hydrogen bond. The bulky side chain is positioned to interfere with the equatorial O4 and this residue is likely to be important for excluding an α-glucoside from subsite +1.

The machinery that stabilizes the O4 and O6 of saccharides in *Bt*GH97b can provide an experimental corroboration of a previously proposed evolutionary relationship of GH97 with GH clan-D [9,14], which consists of GH27, 31, and 36. Superimposition of representative GH clan-D α-galactosidases [15–17] and our crystal structure (Fig. 9B) shows that the machinery for

stabilization of O4 and O6 of α-galactosides is spatially conserved well among GH 27, 36, and 97 α-galactosidases, even though GH27 rice α-galactosidase has a Tyr residue instead of Trp on β-strand 3. The multiple sequence alignment of structure-known GH 27 and 36 α-galactosidases with *Bt*GH97b-D415G, based on a structural alignment by *MATRAS* [18], also indicates conservation of residues associated with stabilization of O4 and O6 of α-galactosides (Fig. 9C). GH31 α-galactosidase possesses a slightly different but highly similar arrangement to accept the axial O4 (Fig. 9B). This enzyme has no corresponding carboxy group to recognize O6, and a Trp486 that interacts with the equatorial O4 is not on the β→α loop 1 but on the β→α loop 8. However, the enzyme has Glu266, Trp305, and Lys363 on the β→α loops 2, 3, and 4, respectively, which stabilize the axial O4, as with GH27, 36, and 97 α-galactosidases. These structural features are obvious proof of the evolutional relationship between GH97 and GH clan-D enzymes.

In this study, we demonstrate that the formate-rescued transglycosylation by *Bt*GH97b-D415G is effective for the synthesis of α-galactosides. Converting a glycosidase to a glycosynthase is a highly respectable strategy to efficiently form glycosidic linkages, but glycosynthases derived from α-glycosidases may fail to generate glycosidic linkages in good yield because of the instability of β-glycosyl fluoride donors. The chemical-rescued transglycosylation using more stable α-glycosyl fluoride substrates could be useful for other α-glycosidases. In addition, our crystal structure complexed with the transglycosylation product offers insight into structure and function relationships in not only GH97 but also GH clan-D enzymes.

Materials and methods

General Procedures

^{1}H NMR spectra were recorded on JEOL JNM-AL400 (400 MHz) or JNM-ECA600 (600 MHz) spectrometers (JEOL Ltd., Tokyo, Japan). ^{13}C (150 MHz), COSY, HSQC, HSQC-TOCSY, and HMBC NMR spectra were recorded on a JEOL JNM-ECA600 spectrometer (JEOL Ltd.). ESI-MS was performed using a Thermo Scientific Exactive spectrometer (Thermo Fisher Scientific, Inc., Waltham, MA, USA). TLC separation of saccharides was performed using 0.25-mm layers of silica gel 60 F_{254} (Merck, Darmstadt, Germany). The reaction mixtures containing a monosaccharide or disaccharide as the acceptor substrate were developed twice using a solvent

system of nitromethane:1-propanol:water (4:10:3, v/v), whereas the reaction mixtures containing PNP glycosides were developed using a solvent system of ethyl acetate:methanol:water (7:2:1, v/v/v). The sugar and sugar derivatives were visualized by spraying with an α-naphthol–sulfuric acid solution (15% sulfuric acid in methanol containing 2.1 mM α-naphthol), followed by heating at 110 °C for 5 min The concentrations of monosaccharides and disaccharides were measured by HPAEC–PAD using a Dionex ICS-3000 system (Dionex/Thermo Fisher Scientific, Idstein, Germany) equipped with a CarboPac PA1 analytical column (4 mm × 250 mm; Dionex/Thermo Fisher Scientific), or by an HPLC system (JASCO, Tokyo, Japan) equipped with Corona charged aerosol detector (ESA Biosciences, Inc., Chelmsford, MA, USA) with a Cosmosil Sugar-D analytical column (4.6 mm × 250 mm; Nacalai Tesque, Kyoto, Japan). For HPAEC-PAD; the column was pre-equilibrated with eluent before each chromatographic analysis. Separation conditions (flow speed, 0.8 mL min^{-1}; sample injection, 10 μL containing internal standard sorbitol) were as follows: for glucose or xylose, isocratic elution with 15 mM NaOH; for lactose or maltose isocratic elution with 160 mM NaOH; for cellobiose, 2-step separation comprising an initial isocratic elution with 15 mM NaOH for 30 min and then gradient elution of 15–160 mM NaOH over 20 min. Sodium hydroxide solutions were prepared from super special grade 50% NaOH solution (Wako Pure Chemical Industries, Ltd., Osaka, Japan). The concentration of each saccharide was calculated using a calibration curve prepared from chromatographic peak areas of sorbitol and concentration-known saccharide standards. Chromatograms were evaluated with *Chromeleon* software (Dionex/Thermo Fisher Scientific). For HPLC; the separation of each saccharide was achieved using a mobile phase (acetonitrile/water, 75:25, v/v) with a flow rate of 1 mL min^{-1} at 30 °C. The chromatograms were processed on a BORWIN/HSS-2000 (JASCO). The concentrations of PNP glycosides were measured by RP-HPLC equipped with a Cosmosil $5C_{18}$-AR-II analytical column (4 mm × 250 mm; Nacalai Tesque) and a mobile phase (acetonitrile/water, 9:93, v/v) with a flow rate of 0.5 mL min^{-1} at 30 °C. Each PNP glycoside was detected by absorbance at 313 nm, and the concentration calculated using a calibration curve prepared from chromatographic peak areas of a concentration-known PNP α-glucoside standards. Methylation analyses were performed as described previously [19,20].

Chemicals

α-GalF was synthesized from 1,2,3,4,6-penta-*O*-acetyl-D-galctopyranose according to a published method [21]. 2,3,4,6-tetra-*O*-acetyl α-D-galactosyl fluoride: ^{1}H NMR (600 MHz, $CDCl_3$) δ (ppm): 5.80 (dd, *J* = 2.7 and 53.4 Hz, 1H, H-1), 5.53 (dd, *J* = 1.1 and 3.2 Hz, 1H, H-4), 5.36 (dd, *J* = 3.2 and 10.9 Hz, 1H, H-3), 5.18 (ddd, *J* = 2.7, 10.9 and 23.8 Hz, 1H, H-2), 4.41 (t, *J* = 6.5 Hz, 1H, H-5), 4.16 (dd, *J* = 6.5 and 11.5 Hz, 1H, H-6a), 4.11 (dd, *J* = 6.8 and 11.5 Hz, 1H, H-6b), 2.15 (s, 3H, OAc), 2.12 (s, 3H, OAc), 2.06 (s, 3H, OAc), 2.01 (s, 3H, OAc). Deacetylation of the 2,3,4,6-tetra-*O*-acetyl α-D-galactosyl fluoride was performed with sodium methoxide in dry methanol to give α-GalF. β-$GalN_3$ and PNP β-mannoside were purchased from Sigma Aldrich (St. Louis, MO, USA) PNP β-glucoside and β-galactoside were purchased from Tokyo Chemical Industry Co., LTD. (Tokyo, Japan). All other chemicals and reagents were purchased from Nacalai Tesque unless indicated otherwise.

Production and purification of *Bt*GH97b-D415G

Production and purification of the recombinant *Bt*GH97b-D415G were carried out as reported previously [11]. *Escherichia coli* BL21(DE3) strain was used as the host for expression. The purity of the recombinant enzyme was confirmed by SDS-PAGE. Protein concentration was estimated by amino acid analysis of the protein hydrolysate (6 M hydrochloric acid, 110 °C, 24 h) using a JLC-500/V (JEOL Ltd.) equipped with a ninhydrin-detection system.

Chemical rescue and transglycosylation kinetics

All kinetic experiments were carried out at 30 °C in 0.1 M 2-morpholinoethanesulfonic acid monohydrate (MES)-NaOH buffer (pH 6.0) containing 120 mM sodium chloride and 20 mM calcium chloride unless otherwise stated. An Orion fluoride ion electrode (model 9609BNWP; Thermo Fisher Scientific) was used to monitor fluoride ion release from α-GalF. Initial rates were determined from linear fits of ion released from 2 to 8 min of the reaction and were used for the determination of kinetic parameters. All enzymatic reaction rates were corrected by subtracting the spontaneous hydrolysis rate of α-GalF. Kinetic parameters were obtained by direct fit of the data from reactions, where concentration of α-GalF was varied in the presence (100 mM) or absence of lactose, to the Michaelis–Menten equation using the computer program *GraFit 7* (Erithacus Software Ltd, Surrey, UK). The enzyme concentrations used were 160 nM (w/ sodium

formate), 8.2 nM (w/ sodium azide, w/o lactose), and 160 nM (w/ sodium azide, w/ lactose), where the terms w/ and w/o indicate with and without, respectively. The acceptor-dependent initial liberation rates of fluoride ion were measured at a fixed concentration of α-GalF (10 mM) using various concentrations of acceptors (lactose, glucose, xylose, galactose, maltose, and cellobiose) with an enzyme concentration of 320 nM. Initial rates were fit according to equation 2, $[v/[E]_0 = (\alpha + \beta[S_2])/(\gamma + [S_2])]$, where $[S_2]$ represents the acceptor concentration.

Analysis of products from an azide rescue reaction

The enzymatic reactions were performed using a solution of 1.2 μM *Bt*GH97b-D415G, 20 mM α-GalF, and 300 mM sodium azide in a final volume of 1 mL of 100 mM MES-NaOH buffer with 120 mM sodium chloride (pH 6.0). The reaction mixtures were incubated at 30 °C for 48 h. The mixtures were heated, lyophilized, and re-dissolved in water. Molecular masses of analytes were confirmed by ESI-MS. ^{1}H NMR samples were prepared by repeated freeze drying and dissolving in D_2O. β-Galactopyranosyl azide: ^{1}H-NMR (400 MHz, D_2O) δ (ppm): 4.66 (1H, d, *J* = 8.7 Hz, H-1), 3.96 (1H, d, *J* = 3.5 Hz, H-4), 3.80 (1H, dd, *J* = 7.3 Hz, 15.6 Hz, H-6), 3.79 (1H, m, H-5), 3.75 (1H, dd, *J* = 8.8, 15.6 Hz, H-6), 3.68 (1H, dd, *J* = 3.2, 9.6 Hz, H-3), 3.51 (1H, dd, *J* = 9.6, 8.7 Hz, H-2); MS: *m*/*z* calcd: 228.1 $[M+Na]^+$; found: 228.1.

Preparative-scale production, purification, and characterization of oligosaccharides

Oligosaccharides were synthesized using 20 mM of an acceptor, 20 mM α-GalF, and 100 mM sodium formate incubated with 1.2 μM *Bt*GH97b-D415G in 2 mL of 100 mM MES-NaOH (pH 6.0, 120 mM sodium chloride and 20 mM calcium chloride) at 30 °C for 48 h. The reaction solutions were desalted by Amberlite™ MB-4 resin (Organo Co., Tokyo, Japan), lyophilized, and re-dissolved in 75% (v/v) acetonitrile solution. The reaction products were loaded on a Cosmosil Sugar-D column and isocratically eluted at a flow rate of 1 mL min^{-1} in 75% (v/v) acetonitrile:water. Analytes were detected with a refractive index monitor (Jasco RI-2031). Product fractions were evaporated to dryness. The molecular masses of oligosaccharide products were confirmed by ESI-MS. ^{1}H, ^{13}C, and two-dimensional NMR analyses were performed for the main products of reactions using glucose, xylose, or lactose as the acceptor. The main products

from maltose and cellobiose were analyzed by ^{1}H NMR.

β-D-Glucopyranosyl α-D-galactopyranoside [β-D-Glc*p*-(1↔1)-α-D-Gal*p*]: ^{1}H NMR (600 MHz, D_2O) δ (ppm): 5.26 (d, *J* = 3.4 Hz, 1H, H-1), 4.65 (d, *J* = 7.6 Hz, 1H, H-1′), 4.19 (brd, *J* = 5.8 and 6.8 Hz, 1H, H-5), 4.01 (d, *J* = 2.8 Hz, 1H, H-4), 3.89 (m, 1H, H-3), 3.88 (m, 1H, H-6a′), 3.86 (dd, *J* = 3.4 and 10.3 Hz, 1H, H-2), 3.71 (dd, *J* = 3.1 and 6.2 Hz, 1H, H-6b′), 3.70 (brd, *J* = 7.6 Hz, 2H, H-6), 3.53 (dd, *J* = 9.6 and 10.3 Hz, 1H, H-4′), 3.49 (ddd, *J* = 2.1, 6.2, and 10.3 Hz, 1H, H-5′), 3.41 (dd, *J* = 9.6 and 9.6 Hz, 1H, H-3′), 3.39 (dd, *J* = 7.6 and 9.6 Hz, 1H, H-2′); ^{13}C NMR (150 MHz, D_2O) δ (ppm): 106.0 (C-1′), 103.1 (C-1), 79.1 (C-5′), 78.2 (C-4′), 76.0 (C-3′), 74.6 (C-5), 72.3 (C-2′), 72.1(C-3), 72.1 (C-4), 71.2 (C-2), 64.0 (C-6), 63.6 (C-6′); MS: *m*/*z* calcd: 365.1 $[M+Na]^+$; found: 365.1.

α-D-galactopyranosyl-(1→4)-D-xylopyranose, [α-D-Gal*p*-(1→4)-D-Xyl*p*]: ^{1}H NMR (600 MHz, D_2O) δ (ppm): 5.19 (d, *J* = 3.4 Hz, 1H, H-1, α), 5.17 (d, *J* = 3.4 Hz, 1H, H-1′), 4.57 (d, *J* = 7.6 Hz, 1H, H-1, β), 4.17 (dd, *J* = 5.2 and 11.5 Hz, 1H, H-5eq, β), 3.97 (d, *J* = 2.1 Hz, 1H, H-4′), 3.96 (m, 1H, H-5′), 3.93 (m, 1H, H-5, α), 3.85 (dd, *J* = 9.6 and 10.3 Hz, 1H, H-3, α), 3.85 (dd, *J* = 3.4 and 6.1 Hz, 1H, H-2′), 3.85 (m, 1H, H-3′), 3.79 (m, 1H, H-5, α), 3.74 (m, 2H, H-6′), 3.67 (m, 1H, H-4), 3.65 (dd, *J* = 9.9 and 10.0 Hz, 1H, H-3, β), 3.57 (dd, *J* = 3.4 and 9.6 Hz, 1H, H-2, α), 3.42 (dd, *J* = 10.3 and 11.5 Hz, 1H, H-5, β), 3.27 (dd, *J* = 8.2 and 9.9 Hz, 1H, H-2, β); ^{13}C NMR (150 MHz, D_2O) δ (ppm): 103.1 (C-1′), 99.3 (C-1, β), 94.8 (C-1, α), 80.8 (C-4), 77.7 (C-3, β), 76.7 (C-2, β), 74.5 (C-3, α), 74.2 (C-5′), 74.0 (C-2, α), 72.1 (C-2′), 72.1 (C-4′), 71.3 (C-3′), 67.1 (C-5, β), 64.1 (C-6′), 67.1 (C-5, β); MS: *m*/*z* calcd: 335.1 $[M+Na]^+$; found: 335.1.

β-lactosyl α-D-galactopyranoside, [β-D-Glc*p*-(1→4)-β-D-Glc*p*-(1↔1)-α-D-Gal*p*)]: ^{1}H NMR (600 MHz, D_2O) δ (ppm): 5.27 (d, *J* = 3.8 Hz, 1H, H-1), 4.68 (d, *J* = 8.2 Hz, 1H, H-1′), 4.45 (d, *J* = 8.2 Hz, 1H, H-1″), 4.19 (brd, *J* = 6.3, 1H, H-5), 4.02 (d, *J* = 3.3 Hz, 1H, H-4), 3.95 (dd, *J* = 2.3 and 12.1 Hz, 1H, H-6a′), 3.93 (d, *J* = 3.3 Hz, 1H, H-4″), 3.86 (dd, *J* = 3.8 and 10.4 Hz, 1H, H-2), 3.80 (dd, *J* = 5.2 and 12.1 Hz, 1H, H-6b′), 3.80 (m, 1H, H-6a″), 3.78 (brd, *J* = 4.9 and 12.7 Hz, 1H, H-6b″), 3.85 (m, 1H, H-3′), 3.74 (m, 1H, H-6a), 3.73 (m, 1H, H-6b), 3.73 (m, 1H, H-5″), 3.70 (dd, *J* = 8.8 and 9.3 Hz, 1H, H-3′), 3.67 (dd, *J* = 3.3 and 10.2 Hz, 1H, H-3″), 3.66 (dd, *J* = 8.8 and 9.3 Hz, 1H, H-4′), 3.63 (m, H-5′), 3.55 (dd, *J* = 8.2 and 10.2 Hz, 1H, H-2″); ^{13}C NMR (150 MHz, D_2O) δ (ppm): 105.8 (C-1″), 105.4 (C-1′), 103.2 (C-1), 81.1 (C-4′), 78.2 (C-5″), 77.9 (C-5′), 76.9 (C-3′), 75.7 (C-2′), 75.4 (C-3″), 74.6 (C-5), 73.8 (C-2″), 72.1 (C-3), 72.1 (C-4),

71.4 (C-4″), 71.2 (C-2), 64.0 (C-6), 63.9 (C-6″), 63.0 (C-6′); MS: *m*/*z* calcd: 527.2 $[M+Na]^+$; found: 527.2.

The cellobiose-derived mixture of oligosaccharides was treated with β-glucosidase from sweet almond (32 U mL^{-1}; Toyobo Co., Ltd., Biochemical Department, Osaka, Japan) at 37 °C for 96 h. The resultant solution was desalted by Amberlite™ MB4 resin and loaded to a Cosmosil Sugar-D column. Analytes were separated using the procedure mentioned above.

Crystallization, data collection, structure determination, and refinement

The crystals of *Bt*GH97b-D415G complexed with Gal-Lac were obtained by co-crystallization of BtGH97b-D415G with Gal-Lac using the hanging drop vapor diffusion method, in which a drop consisting of 1 μL of protein solution (90 μM) and 1 μL of reservoir solution (100 mM MES-NaOH buffer, pH 6.2, containing 12% (w/v) PEG6000, and 3.9 mM Gal-Lac) was equilibrated against the reservoir solution at 15 °C. X-ray diffraction data of the crystal were collected on beamline BL-5A at Photon Factory, KEK (Tsukuba, Japan) at a wavelength of 1.0000 Å using a Q315r CCD detector (ADSC, Poway, CA, USA). The dataset was collected from a single crystal under a stream of nitrogen at 100 K. The diffraction data set was indexed, integrated, and scaled with the *XDS* program [22]. The crystal exhibited a $P2_12_12_1$ space group with the cell dimensions a = 60.62 Å, b = 100.62 Å, and c = 237.08 Å and diffracted to 1.94 Å resolution. The structure was determined by the molecular replacement method with *phenix.automr* software [23,24] using the protein coordinates of chain A of GH97 retaining the α-galactosidase structure (Protein Data Bank code: 3A24) as a search model. Two molecules were located in the asymmetric unit with a translation function *Z*-score of 39.7. The refinement was converged by several cycles of manual model corrections with *Coot* software [25] and further refined using the *phenix.refine* program [26]. Ramachandran plot analysis was performed using *MolProbity* software [27]. Coordinates and structure factors have been deposited in the Protein Data Bank under accession code 5E1Q. Data processing and refinement statistics are given in Table 4.

Acknowledgments: We thank the staff of the Instrumental Analysis Division of the Creative Research Institution at Hokkaido University for amino acid analysis and mass spectrometric analysis and the staff of the High-resolution NMR Laboratory in the Faculty of Science at

Hokkaido University for NMR analysis. We also thank the staff of beamline BL-5A at Photon Factory, KEK. This work was supported by Japan Society for the Promotion of Science KAKENHI Grants Nos. 20780068 and 26450114.

Author contributions: MO conceived and coordinated the study, performed the experiments for determination of carbohydrate structures, analyzed data, and wrote the paper. KW and KM performed the kinetic experiments. TT and KY performed the crystal structure analysis. AK, MM and PK provided technical assistance. MY, HM, and AK provided essential equipment and facilities. All authors reviewed the results and approved the final version of this manuscript.

References

1. Hancock SM, Vaughan MD & Withers SG (2006) Engineering of glycosidases and glycosyltransferases. *Curr Opin Chem Biol* **10**, 509–519.

2. Mackenzie LF, Wang Q, Warren RAJ & Withers SG (1998) Glycosynthases: Mutant glycosidases for oligosaccharide synthesis. *J Am Chem Soc* **120**, 5583–5584.

3. Williams SJ & Withers SG (2000) Glycosyl fluorides in enzymatic reactions. *Carbohydr Res* **327**, 27–46.

4. Okuyama M, Mori H, Watanabe K, Kimura A & Chiba S (2002) α-Glucosidase mutant catalyzes "α-glycosynthase"-type reaction. *Biosci Biotechnol Biochem* **66**, 928–33.

5. Cobucci-Ponzano B, Zorzetti C, Strazzulli A, Carillo S, Bedini E, Corsaro MM, Comfort DA, Kelly RM, Rossi M & Moracci M (2011) A novel α-D-galactosynthase from Thermotoga maritima converts β-D-galactopyranosyl azide to α-galacto-oligosaccharides. *Glycobiology* **21**, 448–456.

6. Cobucci-Ponzano B, Conte F, Bedini E, Corsaro MM, Parrilli M, Sulzenbacher G, Lipski A, Dal Piaz F, Lepore L, Rossi M & Moracci M (2009) β-Glycosyl azides as substrates for α-glycosynthases: Preparation of efficient α-L-Fucosynthases. *Chem Biol* **16**, 1097–1108.

7. Moracci M, Trincone A, Perugino G, Ciaramella M & Rossi M (1998) Restoration of the activity of active-site mutants of the hyperthermophilic β-glycosidase from Sulfolobus solfataricus: dependence of the mechanism on the action of external nucleophiles. *Biochemistry* **37**, 17262–17270.

8. Ly HD & Withers SG (1999) Mutagenesis of glycosidases. *Annu Rev Biochem* **68**, 487–522.

9. Gloster TM, Turkenburg JP, Potts JR, Henrissat B & Davies GJ (2008) Divergence of catalytic mechanism within a glycosidase family provides insight into evolution of carbohydrate metabolism by human gut flora. *Chem Biol* **15**, 1058–1067.

10. Kitamura M, Okuyama M, Tanzawa F, Mori H, Kitago Y, Watanabe N, Kimura A, Tanaka I & Yao M (2008) Structural and functional analysis of a glycoside hydrolase family 97 enzyme from Bacteroides thetaiotaomicron. *J Biol Chem* **283**, 36328–37.

11. Okuyama M, Kitamura M, Hondoh H, Kang M-S, Mori H, Kimura A, Tanaka I & Yao M (2009) Catalytic mechanism of retaining α-galactosidase belonging to glycoside hydrolase family 97. *J Mol Biol* **392**, 1232–1241.

12. Cleland WW (1975) Partition analysis and concept of net rate constants as tools in enzyme kinetics. *Biochemistry* **14**, 3220–3224.

13. Cuskin F, Lowe EC, Temple MJ, Zhu Y, Cameron EA, Pudlo NA, Porter NT, Urs K, Thompson AJ, Cartmell A, Rogowski A, Hamilton BS, Chen R, Tolbert TJ, Piens K, Bracke D, Vervecken W, Hakki Z, Speciale G, Munōz-Munōz JL, Day A, Peña MJ, McLean R, Suits MD, Boraston AB, Atherly T, Ziemer CJ, Williams SJ, Davies GJ, Abbott DW, Martens EC & Gilbert HJ (2015) Human gut Bacteroidetes can utilize yeast mannan through a selfish mechanism. *Nature* **517**, 165–169.

14. Naumoff DG (2005) GH97 is a new family of glycoside hydrolases, which is related to the α-galactosidase

superfamily. *BMC Genomics* **6**, 112.
15. Fujimoto Z, Kaneko S, Momma M, Kobayashi H & Mizuno H (2003) Crystal structure of rice alpha-galactosidase complexed with D-galactose. *J Biol Chem* **278**, 20313–20318.
16. Fredslund F, Hachem MA, Larsen RJ, Sorensen PG, Coutinho PM, Lo Leggio L & Svensson B (2011) Crystal structure of α-galactosidase from Lactobacillus acidophilus NCFM: insight into tetramer formation and substrate binding. *J Mol Biol* **412**, 466–480.
17. Miyazaki T, Ishizaki Y, Ichikawa M, Nishikawa A & Tonozuka T (2015) Structural and biochemical characterization of novel bacterial α-galactosidases belonging to glycoside hydrolase family 31. *Biochem J* **469**, 145–158.
18. Kawabata T (2003) MATRAS: a program for protein 3D structure comparison. *Nucleic Acids Res* **31**, 3367–3369.
19. Song KM, Okuyama M, Kobayashi K, Mori H & Kimura A (2013) Characterization of a glycoside hydrolase family 31 α-glucosidase involved in starch utilization in Podospora anserina. *Biosci Biotechnol Biochem* **77**, 2117–2124.
20. Mukerjea R, Kim D & Robyt JF (1996) Simplified and improved methylation analysis of saccharides, using a modified procedure and thin-layer chromatography. *Carbohydr Res* **292**, 11–20.
21. Hayashi M, Hashimoto S & Noyori R (1984) Simple synthesis of glycosyl fluoride. *Chem Lett* **10**, 1747–1750.
22. Kabsch W (2010) XDS. *Acta Crystallogr D Biol Crystallogr* **66**, 125–132.
23. Adams PD, Afonine P V, Bunkoczi G, Chen VB, Davis IW, Echols N, Headd JJ, Hung LW, Kapral GJ, Grosse-Kunstleve RW, McCoy AJ, Moriarty NW, Oeffner R, Read RJ, Richardson DC, Richardson JS, Terwilliger TC & Zwart PH (2010) PHENIX: a comprehensive Python-based system for macromolecular structure solution. *Acta Crystallogr D Biol Crystallogr* **66**, 213–221.
24. McCoy AJ, Grosse-Kunstleve RW, Adams PD, Winn MD, Storoni LC & Read RJ (2007) Phaser crystallographic software. *J Appl Crystallogr* **40**, 658–674.
25. Emsley P, Lohkamp B, Scott WG & Cowtan K (2010) Features and development of Coot. *Acta Crystallogr D Biol Crystallogr* **66**, 486–501.
26. Afonine P V, Grosse-Kunstleve RW, Echols N, Headd JJ, Moriarty NW, Mustyakimov M, Terwilliger TC, Urzhumtsev A, Zwart PH & Adams PD (2012) Towards automated crystallographic structure refinement with phenix.refine. *Acta Crystallogr D Biol Crystallogr* **68**, 352–367.
27. Chen VB, Arendall 3rd WB, Headd JJ, Keedy DA, Immormino RM, Kapral GJ, Murray LW, Richardson JS & Richardson DC (2010) MolProbity: all-atom structure validation for macromolecular crystallography. *Acta Crystallogr D Biol Crystallogr* **66**, 12–21.

Table 1. Transglycosylation by *Bt*GH97b-D415G.

Reactions were performed at 30 °C for 48 h in 0.1 M MES-NaOH buffer (pH 6.0) containing 120 mM sodium chloride and 20 mM calcium chloride. [a] Reaction mixtures contained 40 mM α-GalF and 20 mM acceptor substrate. [b] Reaction mixtures contained 20 mM α-GalF and 10 mM acceptor substrate. [c] Reaction mixtures contained 20 mM β-$GalN_3$ and 20 mM acceptor substrate. [d] Reaction mixtures contained 10 mM β-$GalN_3$ and 10 mM acceptor substrate. [e] Yields were calculated from the consumption of acceptor molecule. [f] The consumption of lactose was too little to detect when lactose was used as an acceptor in the azide-rescue reaction. The linkage formed was determined by NMR analyses. [g] The linkage formed was determined by methylation analysis.

Donor	Nucleophile	Acceptor	Yield (%) [e]	Linkage of a main product
α-GalF	100 mM formate	Glucose [a]	75	α(1↔1)β [g]
		Xylose [a]	90	α(1→4) [g]
		Cellobiose [a]	75	α(1↔1)β, α(1→6) [h]
		Lactose [a]	85	α(1↔1)β [g]
		Maltose [a]	75	α(1↔1)β [g]
		PNP α-glucoside [b]	95	α(1→6) [h]
		PNP β-glucoside [b]	89	α(1→6) [h]
		PNP α-mannoside [b]	92	
		PNP β-mannoside [b]	73	
α-GalF	300 mM azide	Glucose [a]	28	
		Xylose [a]	25	
		Cellobiose [a]	42	
		Lactose [a]	– [f]	
		Maltose [a]	8	
		PNP α-glucoside [b]	18	
		PNP β-glucoside [b]	13	
		PNP α-mannoside [b]	23	
		PNP β-mannoside [b]	24	
β$GalN_3$		Glucose [c]	45	
		Xylose [c]	47	
		Cellobiose [c]	39	
		Lactose [c]	36	
		Maltose [c]	16	
		PNP α-glucoside [d]	18	
		PNP β-glucoside [d]	29	
		PNP α-mannoside [d]	43	
		PNP β-mannoside [d]	22	

Table 2. Kinetic parameters for reaction of *Bt*GH97b-D415G.

Reactions were carried out at 30 °C in 0.1 M MES-NaOH buffer (pH 6.0) containing 120 mM sodium chloride, 20 mM calcium chloride, varying [α-GalF], and with or without 100 mM lactose.

Nucleophile	100 mM lactose	K_m (mM)	k_{cat} (s^{-1})	k_{cat}/K_m ($s^{-1}\cdot mM^{-1}$)
100 mM	−	0.136 ± 0.026	0.236 ± 0.006	1.77 ± 0.29
Formate	+	0.146 ± 0.003	0.322 ± 0.009	2.21 ± 0.02
100 mM	−	0.101 ± 0.024	1.65 ± 0.15	16.7 ± 2.3
Azide	+	0.161 ± 0.007	0.316 ± 0.003	1.96 ± 0.08

Table 3. Transglycosylation reaction kinetics for *Bt*GH97b-D415G with various acceptors.

Acceptors of various concentrations were incubated with *Bt*GH97b-D415G, 10 mM α-GalF, and an external nucleophile (100 mM sodium formate or 300 mM sodium azide) in 0.1 M MES-NaOH buffer (pH 6.0) containing 120 mM sodium chloride and 20 mM calcium chloride. Initial rates of fluoride ion release are fitted to equation 2, $v/[E]_0 = (\alpha + \beta[S_2])/(\gamma + [S_2])$, where $[S_2]$ represents the acceptor concentration. The parameters, α, β, and γ, indicate $k_2k_3K_{m2}/(k_2 + k_5)$, $k_2k_5/(k_2 + k_5)$, and $(k_2 + k_3)K_{m2}/(k_2 + k_5)$, respectively, when there is a sufficient amount of α-GalF ([α-GalF] >> K_m).

Acceptor	Nucleophile	α	β	γ	α/γ	β/α
Lactose	Formate	1.34 ± 0.24	0.327 ± 0.026	15.0 ± 2.0	0.0893	0.244
Lactose	Azide	71.7 ± 2.7	0.0103 ± 0.043	27.3 ± 0.7	2.63	0.144×10^{-3}
Xylose	Formate	2.47 ± 0.36	0.481 ± 0.039	34.9 ± 2.5	0.0708	0.195
Glucose	Formate	9.51 ± 0.16	0.567 ± 0.006	63.8 ± 6.0	0.149	0.0596
Maltose	Formate	2.19 ± 0.15	0.311 ± 0.029	31.1 ± 6.1	0.0704	0.142
Cellobiose	Formate	0.658 ± 0.087	0.246 ± 0.012	8.63 ± 0.27	0.0762	0.374

Table 4. Data collection and refinement statistics for datasets of *Bt*GH97b-D415G complex with Gal-Lac.

Space group	$P2_12_12_1$
Unit cell parameters (*a*, *b*, *c*; Å)	60.62, 100.62, 237.08
Resolution range (Å)	50–1.94 (2.06–1.94)
No. of unique reflections	106969 (16428)
R_{meas}	0.089 (1.076)
Completeness (%)	99.2 (95.5)
$\langle I/\sigma(I)\rangle$	18.40 (2.31)
Multiplicity	7.3 (7.3)
Refinement	
R_{work}	0.1853
R_{free}	0.2225
No. of protein atoms	10253
No. of sugar atoms	68
No. of glycerol atoms	18
No. of water molecules	763
No. of Ca ions	2
Averaged B-factors	
Protein	42.9
Sugar	31.7
Glycerol	46.2
Water	41.9
Ca ion	27.6
R.m.s.d. from ideal values	
Bond lengths (Å)	0.008
Bond angles (°)	1.079
Ramachandran plot analysis	
Favored region (%)	96.88
Allowed region (%)	2.96
Outlier region (%)	0.16

Figure legends

Fig. 1. Plots of initial reaction velocity *versus* concentration of external nucleophiles for the *Bt*GH97b-D415G catalyzed reaction of α-GalF.

Reactions (20 mM α-GalF and 1.6 μM of *Bt*GH97b-D415G) were performed using various concentrations (0–500 mM) of external nucleophiles (A) sodium formate or (B) sodium azide, in 100 mM MES-NaOH (120 mM sodium chloride and 20 mM calcium chloride, pH 6.0). Fluoride ion released from α-GalF was monitored by a fluoride ion electrode. Experiments were repeated three times and average values are plotted (error bar, S.D.).

Fig. 2. Chemical rescue reaction catalyzed by *Bt*GH97b-D415G in the presence of 20 mM lactose and 20 mM α-GalF.

A, TLC analysis of the reaction mixtures containing α-GalF, lactose, 100 mM of each external nucleophile anion, and *Bt*GH97b-D415G (4.8 μM) in 100 mM MES-NaOH (120 mM sodium chloride and 20 mM calcium chloride, pH 6.0) that were incubated at 30 °C for 48 h. The TLC shows reaction mixtures without any nucleophilic anion (lane 1), with formate (lane 2), azide (lane 3), and acetate (lane 4); and reference spots of α-GalF (lane F), β-galactosyl azide (lane N), galactose (lane G), and lactose (lane L). B, Estimation of the concentrations of oligosaccharides synthesized. Each reaction mixture with the same composition as panel A was incubated at 30 °C. An aliquot of each reaction mixture was taken at each time point and the concentration of Gal-Lac estimated from the consumption of lactose, which was determined by HPAEC–PAD. Traces show reactions without any nucleophilic anion (open diamonds), with formate (closed circles); with azide (open squares); and with acetate (open triangles).

Fig. 3. Glycosynthase kinetics with *Bt*GH97b-D415G.

A; various concentrations (0.2–2.4 mM) of β-GalN_3 were incubated with *Bt*GH97b-D415G (4.0 μM) and 100 mM lactose at pH 6.0 and 30 °C. The reaction rate was determined by the increase in the transfer product. The concentration of the product was measured by HPAEC–PAD. Data points were fitted with a Michaelis–Menten equation. B; various concentrations (10–100 mM) of lactose and β-GalN_3 fixed at 10 mM were incubated with *Bt*GH97b-D415G (4.0 μM) at pH 6.0 and 30 °C. The reaction rate was calculated using the concentration of the transfer product, which was quantified by HPAEC–PAD. Experiments were repeated three times and average values are plotted (error bar, S.D.).

Fig. 4. NMR spectra of oligosaccharides.

A, B, and C; Sections of HMBC spectra of β-D-Glc*p*-(1↔1)-α-D-Gal*p*, α-D-Gal*p*-(1→4)-D-Xyl*p*, and β-D-Gal*p*(1→4)-β-D-Glc*p*-(1↔1)-α-D-Gal*p*, respectively. D, ^{1}H-NMR spectrum of the major product from α-GalF and maltose (range, 4.6–5.5 ppm) with the relative integral values (red).

Fig. 5. Structural analysis of oligosaccharides from reaction with cellobiose as the acceptor.

A, ^{1}H-NMR spectrum of oligosaccharides (range from 4.3 to 5.4 ppm) with the relative integral values (red). B, HPLC analysis of the hydrolysate by β-glucosidase (chromatogram a). Standards of glucose and β-D-Glc*p*-(1↔1)-α-D-Gal*p* are shown in chromatograms b and c, respectively. The oligosaccharide insusceptible to β-glucosidase is indicated by the arrow. C, TLC analysis of hydrolysates of methylated maltose (lane 1), isomaltose (lane 2), isomaltotriose (lane 3), lactose (lane 4), and the β-glucosidase-insusceptible oligosaccharide (lane 5). TLC compound identification: d, 2,3,4,6-tetra-*O*-methyl-glucose; e, 2,3,4,6-tetra-*O*-methyl-galactose; f, 2,3,6-tri-*O*-methyl-glucose; and g, 2,3,4-tri-*O*-methyl-glucose.

Fig. 6. Plots of initial reaction rates *versus* substrate concentration for the *Bt*GH97b-D415G catalyzed reactions of α-GalF with or without lactose.

A, B; various concentrations (0.05–0.8 mM) of α-GalF were incubated with *Bt*GH97b-D415G and 0 mM (closed circle) or 100 mM lactose (open circle) in the presence of 100 mM sodium formate (A) or 300 mM sodium azide (B), pH 6.0 at 30 °C. Each reaction rate was determined by the increase in fluoride ion concentration. Data points were fitted with a Michaelis–Menten equation. The enzyme concentrations used were 160 nM (A), 8 nM (B in the absence of lactose), and 80 nM (B in the presence of lactose). Rate constants are listed in Table 1. C, D; various concentrations (0–90 mM) of lactose and α-GalF fixed at 10 mM were incubated with *Bt*GH97b-D415G (33 nM) in the presence of 100 mM sodium formate (C) or 300 mM sodium azide (D), pH 6.0 at 30 °C. Each reaction rate was determined by the increase in fluoride ion concentration. Data points were fitted with the equation $v/[E]_0 = (\alpha + \beta[\text{lactose}])/(\gamma + [\text{lactose}])$ (equation 2). Rate constants are listed in Table 2. All experiments were repeated three times and average values are plotted (error bar, S.D.).

Fig. 7. Proposed kinetic scheme for the chemical-rescued transglycosylation catalyzed by the *Bt*GH97b nucleophile mutant.

E, *Bt*GH97b-D415G supplemented with the external nucleophilic anion; S, α-GalF; S_2, acceptor; K_{S2}', the dissociation constant of S_2 from E; P_1, fluoride; P_2, β-galactosyl azide or galactose; P_3, transglycosylation product.

Fig. 8. Crystal structure of *Bt*GH97b-D415G complexed with Gal-Lac.

A, Overall structure of *Bt*GH97b-D415G complexed with Gal-Lac. Domains N, A, and C are shown in *yellow*, *cyan*, and *orange*, respectively (the same colors are also used in other panels). B, F_o - F_c omit map of Gal-Lac and the calcium ion. The contour level is at 3σ. C, Stereo views of hydrogen bonds (dashed lines) with bound

Gal-Lac. D, The structure of positive subsites. Subsite +1 is constricted by His245, Trp312, Phe416, and Trp474. The sugar moiety at subsite +2 is placed on a side chain of Trp474. The figures were rendered by PyMOL (https://www.pymol.org/).

Fig. 9. Structural features of *Bt*GH97b for the recognition of the axial hydroxy groups at C4 and C6.

A, Difference in the recognition of hydroxy groups at C4 and C6 between *Bt*GH97b (left) and *Bt*GH97a (right; pdb id, 2zq0). Hydrogen bonds are shown by dashed lines. B, Comparison of the recognition machinery for hydroxy groups at C4 and C6 in GH97, 27, 31, and 36 α-galactosidases. *Bt*GH97b is displayed in green, the GH27 rice α-galactosidase in cyan (PDB id 1uas), the GH31 *P. saltans* α-galactosidase in yellow (PDB id 4xpp), and *L. acidophilus* α-galactosidase in magenta (PDB id 2xn2). C, Multiple 3D alignment of *Bt*GH97b-D415G, GH27 and 36 α-galactosidases. Among the alignments, regions of the β→α loops 1, 2, 3, and 4 are shown in the figure. The alignment was calculated using the multiple 3D alignment tool in *MATRS* (http://strcomp.protein.osaka-u.ac.jp/matras/) [18]. Four characters on the left side represent PDB ids. Secondary structure elements and residue numbers are of *Bt*GH97b-D415G.

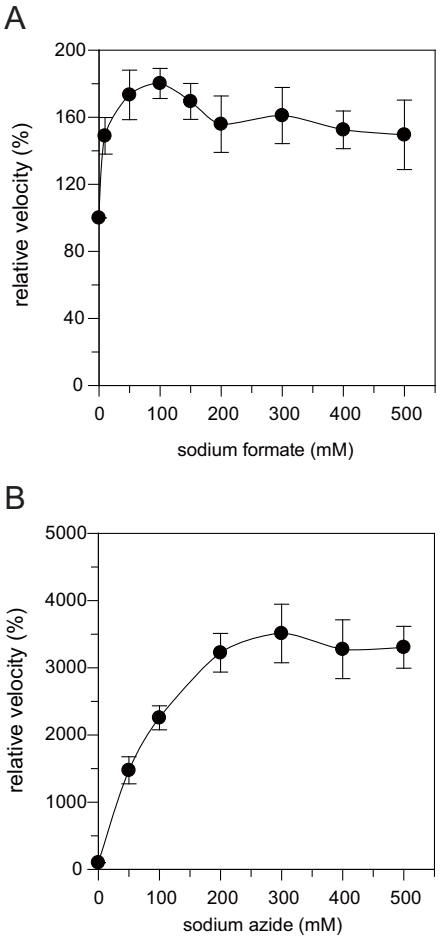

Figure 1 Okuyama *et al*

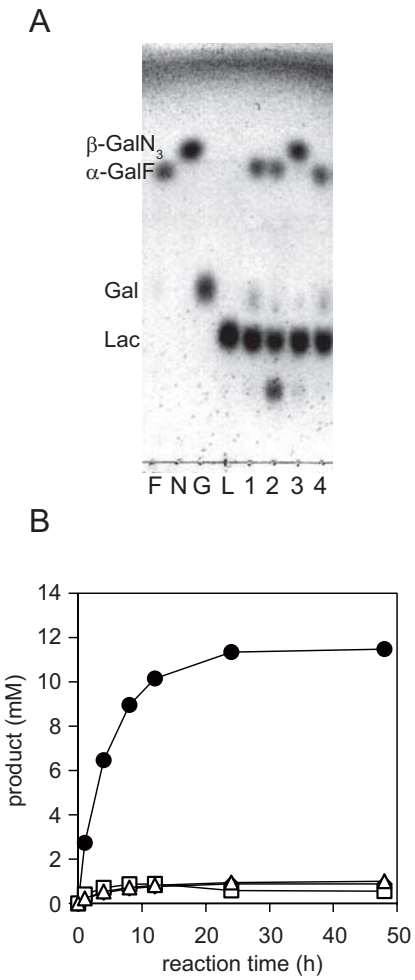

Figure 2 Okuyama *et al*

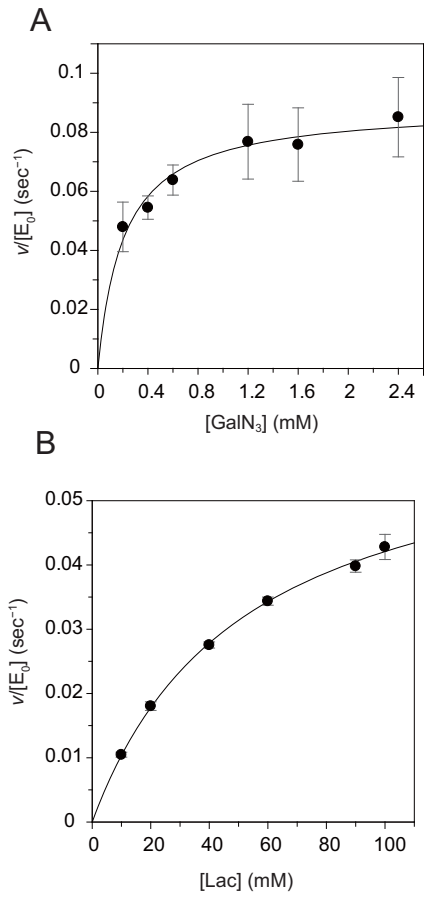

Figure 3 Okuyama *et al*

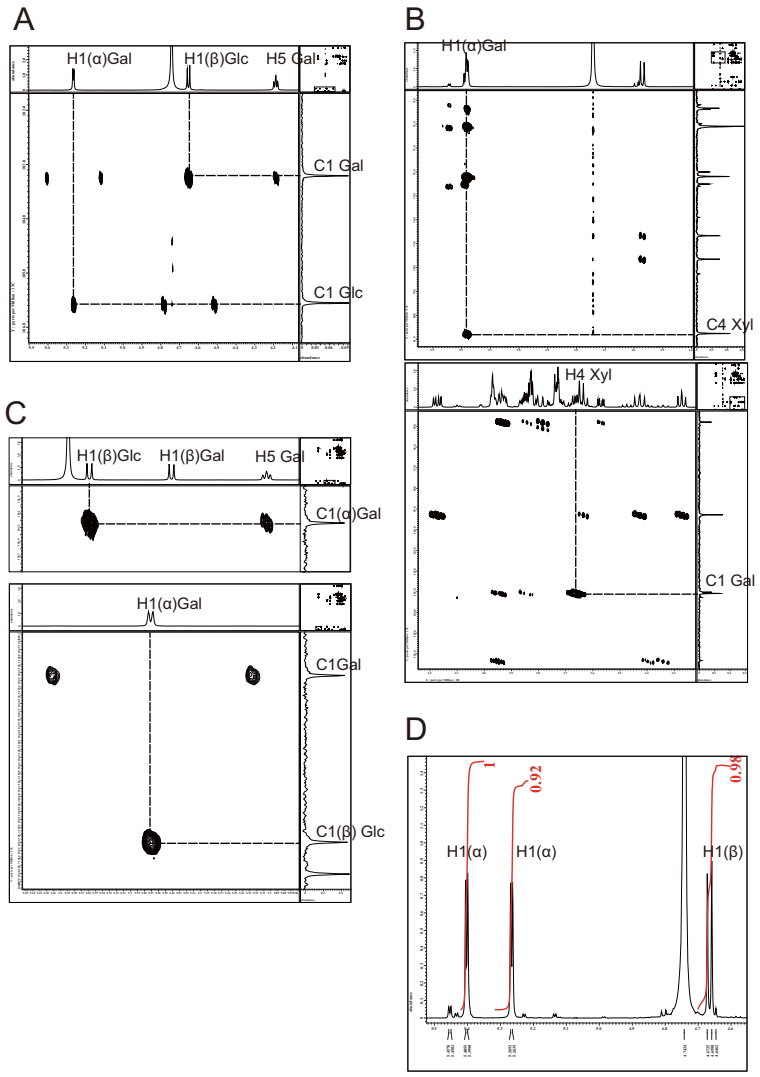

Figure 4 Okuyama *et al*

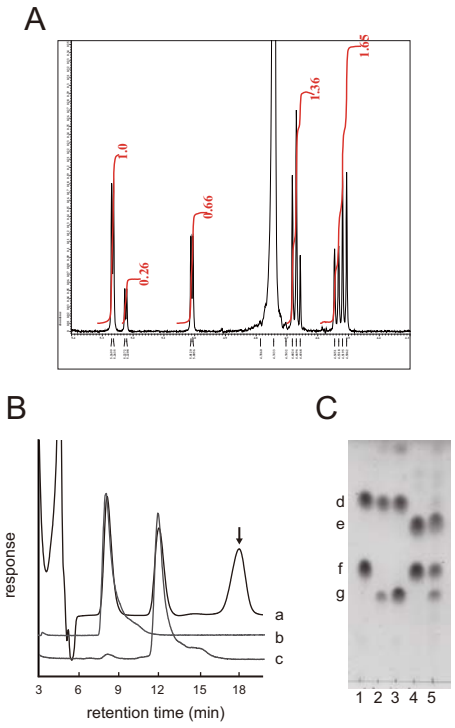

Figure 5 Okuyama *et al*

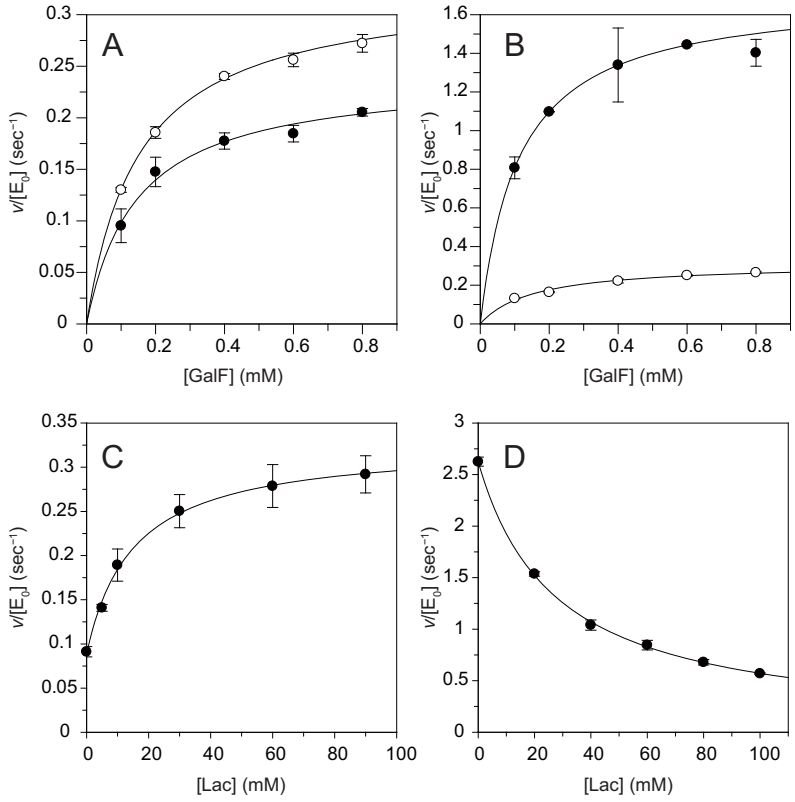

Figure 6 Okuyama *et al*

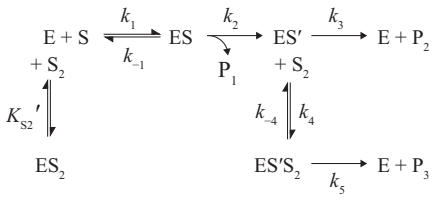

Figure 7 Okuyama *et al*

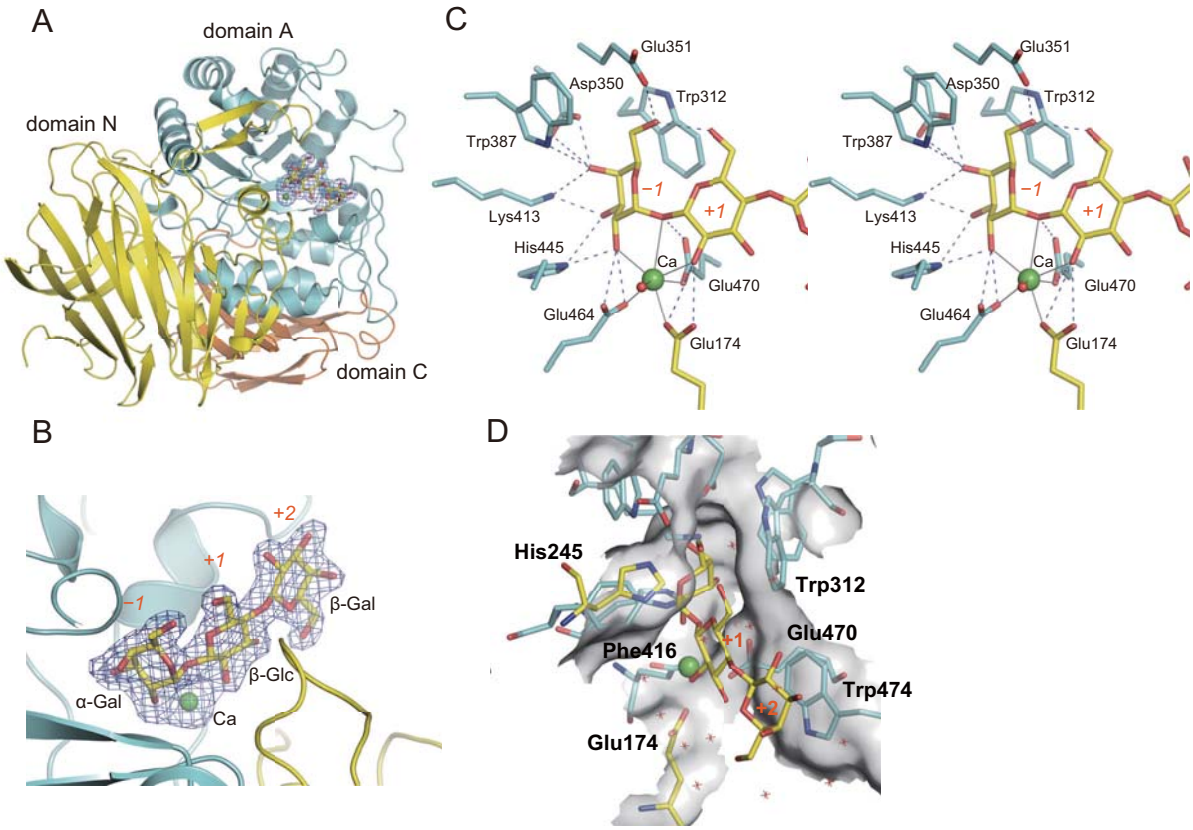

Figure 8 Okuyama *et al*

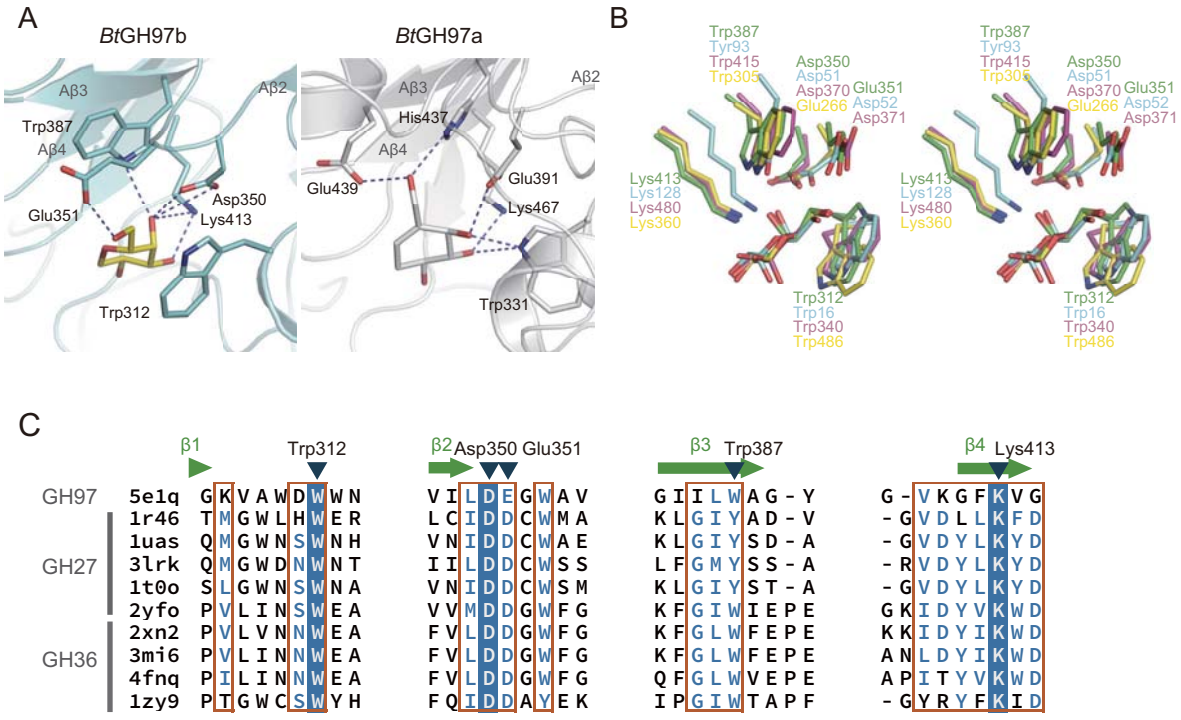

Figure 9 Okuyama *et al*